

1 **Salivary molecular spectroscopy: a rapid and non-invasive monitoring tool for**
2 **diabetes mellitus during insulin treatment**

3

4 CAIXETA, D.C.^{1,2}, AGUIAR, E. M. G.¹, CARDOSO-SOUZA, L.¹, COELHO, L.M.D¹,
5 OLIVEIRA, S.W.¹, ESPINDOLA F.S.², RANIERO L³, CROSARA K.T.B.⁴, BAKER
6 M.J.⁵, SIQUEIRA W.L.⁴, SABINO-SILVA, R. ^{1*}

7 ¹ Department of Physiology, Institute of Biomedical Sciences, Federal University of
8 Uberlandia, Uberlandia, Minas Gerais, Brazil.

9 ² Institute of Genetics and Biochemistry, Federal University of Uberlandia, Uberlandia,
10 Minas Gerais, Brazil.

11 ³ Nanosensor Laboratory, IP&D, University of Vale do Paraíba, São José Dos Campos,
12 SP, Brazil.

13 ⁴ College of Dentistry, University of Saskatchewan, Saskatoon, Saskatchewan, Canada.

14 ⁵ WestCHEM, Department of Pure and Applied Chemistry, Technology & Innovation
15 Centre, University of Strathclyde, Glasgow, G1 1RD, UK.

16

17

18 ***Corresponding Author:**

19 Robinson Sabino-Silva; Federal University of Uberlandia (UFU), Institute of
20 Biomedical Sciences (ICBIM), ARFIS, Av. Pará, 1720, Campus Umuruama, CEP
21 38400-902, Uberlandia, MG, Brazil

22 Phone: +55 34 3218 2100

23 E-mail: robinsonsabino@gmail.com

24

25

26

27

28

29

30

31

32

33 **Abstract:**

34 Monitoring of blood glucose is an invasive, painful and costly practice in diabetes.
35 Consequently, the search for a more cost-effective (reagent-free), non-invasive and
36 specific diabetes monitoring method is of great interest. Attenuated total reflectance
37 Fourier transform infrared (ATR-FTIR) spectroscopy has been used in diagnosis of
38 several diseases, however, applications in the monitoring of diabetic treatment are just
39 beginning to emerge. Here, we used ATR-FTIR spectroscopy to evaluate saliva of non-
40 diabetic (ND), diabetic (D) and diabetic 6U-treated of insulin (D6U) rats to identify
41 potential salivary biomarkers related to glucose monitoring. The spectrum of saliva of
42 ND, D and D6U rats displayed several unique vibrational modes and from these, two
43 vibrational modes were pre-validated as potential diagnostic biomarkers by ROC curve
44 analysis with significant correlation with glycemia. Compared to the ND and D6U rats,
45 classification of D rats was achieved with a sensitivity of 100%, and an average specificity
46 of 93.33% and 100% using bands 1452 cm^{-1} and 836 cm^{-1} , respectively. Moreover, 1452 cm^{-1} and
47 836 cm^{-1} spectral bands proved to be robust spectral biomarkers and highly
48 correlated with glycemia (R^2 of 0.801 and 0.788, $P < 0.01$, respectively). Both PCA-LDA
49 and HCA classifications achieved an accuracy of 95.2%. Spectral salivary biomarkers
50 discovered using univariate and multivariate analysis may provide a novel robust
51 alternative for diabetes monitoring using a non-invasive and green technology.

52

53

54

55

56

57

58

59

60

61

62

63

64

65 **Introduction**

66

67 Diabetes mellitus (DM) is a metabolic disorder characterized by hyperglycemia
68 which results from insufficient secretion and/or reduced insulin action in peripheral
69 tissues (Rolo e Palmeira, 2006; Ashcroft e Rorsman, 2012). According to the
70 International Diabetes Federation (IDF), there are an estimated 425 million adults with
71 diabetes worldwide, these include 212 million whom are estimated undiagnosed (IDF,
72 2017). Frequent monitoring of diabetes is essential for improved glucose control and to
73 delay clinical complications related with diabetes. Besides, the early screening of DM is
74 paramount to reduce the complications of this metabolic disorder worldwide (Uspstf,
75 2008). Despite being relatively invasive and painful, blood analysis per glucometer is
76 currently feasible for screening, monitoring and diagnosing diabetes by needle finger
77 punctures (Dowlaty *et al.*, 2013; Mascarenhas *et al.*, 2014). The constant need of piercing
78 the fingers several times daily by most patients is inconvenient and may lead to the
79 development of finger calluses and difficulty in obtaining blood samples (Dowlaty *et al.*,
80 2013).

81 Saliva reflects several physiological functions of the body (Desai e Mathews,
82 2014; Javaid *et al.*, 2016). In this way, salivary biomarkers might be an attractive
83 alternative to blood for early detection, and for monitoring systemic diseases (Hu *et al.*,
84 2007). Among the advantages, saliva is simple to collect, non-invasive, convenient to
85 store and, compared to blood, requires less handling during clinical procedures. Besides,
86 saliva also contains analytes with real-time monitoring value which can be used to check
87 the individuals condition (Javaid *et al.*, 2016; Zhang *et al.*, 2016). Currently, a broad set
88 of methods are used to analyze saliva including immunoassays, colorimetric, enzymatic,
89 kinetic, chromatographic and mass spectrometric analysis (Saxena *et al.*, 2017). Several
90 studies showed higher salivary glucose levels in DM patients than non-hyperglycemic
91 controls, which suggest that salivary glucose monitoring might be a useful in screening
92 for diabetic patients. However, other studies reject the idea of a direct relationship
93 between salivary glucose and glycemia (Mascarenhas *et al.*, 2014; Gupta, S. *et al.*, 2015;
94 Nunes *et al.*, 2015; Naing e Mak, 2017). A main limitation of salivary-based measurement
95 of glucose for diabetes monitoring is the presence of glucose in foods, which can disturb
96 the monitoring process as it induces changes in salivary glucose concentration. Therefore,
97 other alternatives of salivary monitoring should be studied.

98 Infrared (IR) spectroscopy is emerging as a powerful quantitative and qualitative
99 technique for monitoring characterization of biological molecules in fluids (Bellisola e
100 Sorio, 2012). Attenuated total reflection Fourier-transform infrared (ATR-FTIR)

101 spectroscopy is a global, sensitive and highly reproducible physicochemical analytical
102 technique that identifies structural molecules on the basis of their IR absorption(Ojeda e
103 Dittrich, 2012). Considering that a biomolecule is determined by its unique structure, each
104 one will exhibit a unique ATR-FTIR spectrum, representing the vibrational modes of the
105 constituent structural bonds (Severcan *et al.*, 2010; Ojeda e Dittrich, 2012). ATR-FTIR
106 is a green technology due to processes that eliminate the use of hazardous elements an
107 overarching approach that is applicable to monitoring diseases. The IR spectral modes of
108 biological samples, such as saliva, may be considered as biochemical fingerprints that
109 correlate directly with the presence or absence of diseases, and, furthermore, provide the
110 basis for the quantitative determination of several analytes for monitoring several diseases
111 and to diagnostic interest (Khaustova *et al.*, 2010; Caetano Júnior *et al.*, 2015). The
112 potential of salivary diagnostic for diabetes by IR spectroscopy using barium fluoride
113 (BaF_2) slides was suggested previously (Scott *et al.*, 2010), however, the efficacy of DM
114 monitoring in insulin-treated conditions using ultra-low volumes of saliva remains
115 unknown.

116 In the present study, we tested the hypothesis that non-invasive spectral
117 biomarkers can be identified in saliva of hyperglycemic diabetic and in insulin-treated
118 diabetic rats, and the differentially expressed vibrational modes can be employed as
119 salivary biomarkers for diabetes monitoring. Thus, the aim of our study was to identify
120 infrared spectral signatures of saliva that are suitable to monitoring this metabolic disease
121 in untreated and insulin-treated conditions. For this, the salivary vibrational modes profile
122 of non-diabetic, diabetic and insulin-treated diabetic rats was quantitatively and
123 qualitatively evaluated using univariate and multivariate analysis.

124

125 **Results**

126

127 ***Characterization of diabetes mellitus***

128 To confirm the effectiveness of diabetes induction and insulin treatment, several
129 parameters were assessed in anesthetized animals. As expected, to confirm the diabetic
130 state, table 1 shows that diabetes reduced weight gain ($p < 0.05$), increased water intake
131 ($p < 0.05$) and food ingestion ($p < 0.05$) compared with ND rats. Besides, in diabetic
132 condition, higher plasma glucose ($p < 0.05$), as well as most pronounced urine volume (p
133 < 0.05), associated with higher urine glucose concentration ($p < 0.05$), were observed in
134 D rats compared with ND rats. Insulin treatment contributed to increased ($p < 0.05$)

135 weight gain and decreased water intake ($p < 0.05$) compared with placebo-treated D rats.
136 As expected, insulin treatment decreased plasma glucose ($p < 0.05$), urine volume ($p <$
137 0.05) and urine glucose concentration compared with D rats. Glycemia and urine volume
138 were similar ($p > 0.05$) in ND and D6U animals, indicating that insulin treatment
139 completely reverted hyperglycemia and higher urine volume described in D rats. The
140 insulin treatment promoted a strong reduction in the urinary glucose concentration;
141 however, the urinary glucose concentration was increased ($p < 0.05$) in D6U compared
142 to ND animals.

143

144 ***Average spectra of saliva***

145 A representative infrared average spectrum of saliva from normoglycemic,
146 hyperglycemic and insulin-treated conditions, which contains different molecules such as
147 lipids, proteins, glycoproteins and nucleic acid, are represented in Figure 1. These salivary
148 spectra indicated several differences among non-diabetic, diabetic and insulin-treated
149 diabetic rats. Some bands of interest are shown in figure 1, which contains: asymmetric
150 stretching vibration of CH_2 of acyl chains of lipids (2924 cm^{-1}); amide II (1549 cm^{-1});
151 asymmetric CH_3 bending modes of the methyl groups of proteins (1452 cm^{-1}); amide III
152 band components of proteins (1313 cm^{-1}); mannose-6-phosphate and phosphorylated
153 saccharide residue (1120 cm^{-1}) and C_2 conformation of sugar (836 cm^{-1}).

154

155 ***Spectral bands analyzed by IR spectroscopy***

156 Spectral band areas that indicate the expression of specific molecules were
157 analyzed in saliva. The band area values of 2924 cm^{-1} , 1549 cm^{-1} , 1313 cm^{-1} , 1120 cm^{-1}
158 are presented in supplementary files. Herein, we showed two bands (1452 cm^{-1} and 836 cm^{-1})
159 with a higher potential for diabetes monitoring (Figure 2 and Figure 3,
160 respectively). Representative spectra of 1452 cm^{-1} and 836 cm^{-1} bands are depicted in
161 Figure 2A and 3A. Diabetes induced a decrease ($p < 0.05$) at 1452 cm^{-1} and 836 cm^{-1}
162 bands compared with non-diabetic rats, however, insulin-treated diabetic reverted this
163 alteration in both bands (Figure 2B and 3B, respectively) .

164 To investigate whether these salivary vibrational modes would be reflective of
165 glycemia regulation, these two salivary band areas were discovered to be, via univariate
166 analysis, the best spectral candidates values to indicate the diabetes monitoring in samples
167 with hyperglycemia, normoglycemia and under insulin treatment. Pearson's correlation
168 between these spectral modes (1452 cm^{-1} and 836 cm^{-1}) with glycemia showed high

169 correlation. The both salivary spectral bands presented strong negative correlation with r
170 = -0.801; $p < 0.0001$ for 1452 cm^{-1} (Figure 2C) and $r = -0.788$; $p < 0.0001$ for 836 cm^{-1}
171 (Figure 3C).

172 Considering that sensitivity and specificity are basic characteristics to determine
173 the accuracy of diagnostic and monitoring test, ROC curve analysis were used to evaluate
174 the potential diagnostic of these spectral bands under two conditions of analysis. The first
175 one, we analyzed the condition of normoglycemic (ND and D6U) with hyperglycemic
176 (D). The cutoff value to 1452 cm^{-1} band was 0.405, and the corresponding sensitivity and
177 specificity were 100% and 93.3%, respectively. In ROC analysis, the area under the curve
178 (AUC) of this band was 0.988 (Figure 2D). To emphasizes our focus on insulin-treated
179 rats, we also showed ROC curve analysis comparing only D6U with D. Both sensitivity
180 and specificity of 1452 cm^{-1} band was 100% with cutoff of 0.422 ($p: 0.0027$). Both
181 sensitivity and specificity of 836 cm^{-1} band to differentiate normoglycemic (ND and
182 D6U) than hyperglycemic (D) were 100% with cutoff of 0.128 (Figure 3D). As expected,
183 the ROC curve to differentiate insulin-treated diabetic (D6U) than hyperglycemic (D)
184 showed similar data (Figure 3E).

185

186 ***Differentiation among the groups by Principal Component Analysis followed by
187 linear discriminant analysis (PCA-LDA) and Hierarchical Cluster Analysis (HCA)***

188 Principal component analysis followed by linear discriminant analysis (PCA-
189 LDA) was performed to reduce the dimensionality of the data set, with the preservation
190 of the variance to evaluate the discrimination between the samples. PCA was performed
191 using 6 principal components (PCs), accounting for 95.2% (20/21) of cumulative variance
192 of correct classification with cross validation. The PCA model considered 95.8% of the
193 data of the spectrum through the second derivative for analyze. After linear discriminant
194 analysis (LDA) with leave-one-out cross-validation, three groups (ND, D and D6U) were
195 formed, but only one sample belonging to class D6U was classified for group D (Figure
196 4). Supplementary table 1, Supplementary table 2 and Supplementary table 3 show the
197 mean quadratic distance, discriminant linear function and the summary of classification
198 of each sample (with quadratic distance of each sample, prediction, validation and
199 probability), respectively, in saliva of ND, D and D6U rats.

200 Hierarchical cluster analysis (HCA) was performed to investigate the effects of
201 treatment with insulin on diabetic to the differentiation of non-diabetic and diabetic
202 samples. HCA was performed in part of salivary spectrum. The deconvolution analyzes

203 were done in the five spectral regions represented in Figure 5, as A region (2995 cm^{-1} to
204 2889 cm^{-1}), B region (1664 cm^{-1} to 1581 cm^{-1}), C region (1410 cm^{-1} to 1234 cm^{-1}), D
205 region (1149 cm^{-1} to 1080 cm^{-1}) and E region (1018 cm^{-1} to 955 cm^{-1}) which allowed
206 the differentiation of the non-diabetic, diabetic and insulin-treated diabetic. As seen from
207 the figure 5, all non-diabetics and diabetics were separate with 100% of discrimination.
208 Only one insulin-treated diabetic was categorized as non-diabetic. The total accuracy,
209 which is highly important for potential monitoring applications, was 95.2% (20/21).

210

211 **Discussion**

212

213 The development of a novel, rapid, noninvasive tool for the diagnosis, and the
214 most important, for monitoring diabetes mellitus based on the comprehensive analysis of
215 spectral salivary constituents would be of great use to health clinical. Herein, we have
216 investigated the translational applicability of ATR-FTIR spectroscopy with potential
217 monitoring of metabolic control in diabetes. Six potential spectral bands were detected
218 by ATR-FTIR and, from these, two bands were showed a strong correlation with glycemia
219 and high sensibility and specificity to differentiate hyperglycemic than normoglycemic
220 conditions indicating potential monitoring applicability for diabetes. The discriminatory
221 power of these two salivary ATR-FTIR bands area are candidates for monitoring diabetes
222 under insulin therapy.

223 As expected in diabetic state, plasma glucose, urine volume and urine glucose
224 concentration are increased in non-treated diabetic rats compared to non-diabetic rats. In
225 addition, insulin treatment decreased glycemia, urine volume and urine glucose. These
226 findings are consistent with other studies (Kusari *et al.*, 2007; Eleazu *et al.*,
227 2013)(Sabino-Silva *et al.*, 2009; Diniz Vilela *et al.*, 2016). It is known that salivary
228 composition changes in diabetes mellitus (Rao *et al.*, 2009; Sabino-Silva *et al.*, 2013;
229 Srinivasan *et al.*, 2015). Also, diabetes mellitus frequently decreases salivary flow, alters
230 the expression of salivary proteins and increases glucose levels in saliva (Rao *et al.*, 2009;
231 Bajaj *et al.*, 2012; Sabino-Silva *et al.*, 2013). From these parameters, it is possible to use
232 salivary components to reflect the presence, and severity of hyperglycemia (Rao *et al.*,
233 2015). Saliva of diabetics with poor metabolic control shows an increase in salivary
234 glucose concentration (Abd-Elraheem *et al.*, 2017). The correlation of glycemia with
235 glucose concentration in saliva is still not well established, so currently it is not used to
236 verify the degree of metabolic control and diagnosis in diabetes mellitus (Gupta, A. *et al.*,

237 2015; Kadashetti *et al.*, 2015; Puttaswamy *et al.*, 2017). ATR-FTIR spectroscopy has
238 been used as an alternative discriminatory method to others chronic diseases, due to its
239 major advantages of being label-free and non-destructive, rapid, high-throughput, not
240 requiring sample preparation, and cost effective analytical method for providing details
241 of the chemical composition and molecular structures (Simsek Ozek *et al.*, 2016; Yu *et*
242 *al.*, 2017).

243 The spectral analysis method to dried saliva described in the present study may be
244 used in rodent and human models. Spectral parameters, such as shifts in bands positions
245 and changes in spectral modes intensity can be used to obtain valuable information about
246 sample composition, which may have diagnostic and monitoring potential for many
247 diseases (Severcan *et al.*, 2010). To get relative information about the concentration of
248 the salivary molecules, integrated band area analysis was performed in the saliva spectra
249 since, according to the Beer-Lambert law, absorption band intensity/band area is
250 proportional to the concentration of the sample (Ozek *et al.* 2014; Turker *et al.* 2014).
251 Therefore, differences in the band area for asymmetric CH₃ bending modes of the methyl
252 groups of protein (1452 cm⁻¹) and C₂ endo/anti B-form helix conformation (836 cm⁻¹)
253 differ in salivary constituents among the groups. Bencharit *et al.* (2013) showed the
254 differences on composition of salivary proteins associated with metabolic control in
255 diabetes on a proteomic analysis, and similar quantitative differences were found in the
256 present study analyzed with spectroscopy ATR-FTIR. Type 2 diabetes mellitus induced
257 changes in the lipid and protein components on the erythrocyte membrane and causing
258 structural changes by FTIR spectroscopy in the protein secondary structure with change
259 in the beta-sheet and beta-turn structures (Mahmoud, 2010).

260 These two salivary spectral modes showed a high and significant correlation with
261 the metabolic control. Clinically, the most interesting comparisons are the correlation
262 between these salivary spectral band areas and glycemia. Together, these salivary spectral
263 bands showed a 100% of sensitivity and 100% of specificity in ROC analysis. ROC curve
264 analysis is widely considered to be the most objective and statistically valid method for
265 biomarker performance evaluation (Xia *et al.*, 2013). Regarding the potential for
266 translation to the clinic, our results suggest that two salivary band areas, 1452 cm⁻¹ and
267 836 cm⁻¹ can be considered a non-invasive spectral biomarkers of monitoring diabetes
268 treated with insulin. Different drug treatments and several levels of glucose concentration
269 should ideally be possible to differentiate, therefore more studies need be investigated.
270 These results indicate that these spectral modes can be used as a diagnostic and

271 monitoring platform for diabetes mellitus, once interestingly, insulin treatment was also
272 able to revert the salivary spectra observed in hyperglycemic state. Therefore, insulin
273 treatment is not a potential confounding factor that may influence salivary vibrational
274 mode in comparisons with glycemia. Some studies have indicated specific salivary
275 biomarkers for diabetes, such as glucose, alpha-amylase, immunoglobulins,
276 myeloperoxidases (Zloczower *et al.*, 2007; Rao *et al.*, 2009; Border *et al.*, 2012; Zhang
277 *et al.*, 2016) with similar potential, but not with a focus on disease monitoring and/or with
278 the use of IR spectroscopy.

279 Multivariate analysis as PCA-LDA and HCA can be used to discriminate samples
280 based on their spectrum. In FTIR analysis the diagnostic accuracy for diabetes detection
281 using saliva was 100.0% for the training set and 88.2% for the test (validation) set using
282 linear discriminant analysis (LDA) calculations (Scott *et al.*, 2010). However, in the
283 present study both PCA-LDA and HCA obtained 95.2% of accuracy using saliva to
284 discriminate normoglycemic, diabetic and insulin-treatment diabetic models. It is
285 important emphasizes that our protocol used ultra-low values of saliva (2 μ l) under
286 airflow dried during only 2 minutes and the other study (Scott *et al.*, 2010) used 50 μ l (25
287 times greater) under dried during \sim 30 min at 25 Torr on 13 mm BaF windows. The
288 analysis using univariate analysis was performed only in the present study. Besides, the
289 Pearson's correlation between 1452 cm^{-1} and 836 cm^{-1} vibrational modes with glycemia
290 described in present study showed higher correlation values ($r = 0.801$ and $r = -0.788$)
291 comparing with another study (Scott *et al.*, 2010; $r = 0.49$) using a SCN band, a classical
292 indicator of tobacco smoking (a condition present in \sim 60% healthy and diabetic subjects).

293 Cluster analyses confirm its potential to discriminate ND, D and D6U groups with
294 high accuracy. The success rate for ND e D was 100 %, and for D6U was 85.7%.
295 Altogether, the data performed an accuracy of 95.23%. The inclusion of one sample of
296 D6U animals in non-diabetic control group is expected considering that insulin is a gold-
297 standard treatment of diabetes. We believe that this infrared analysis open perspectives to
298 use saliva to monitor the metabolic control with molecules different than glucose. It is
299 unequivocal that glucose is the main molecule to monitoring metabolic control in blood,
300 however, the demonstration of glucose transporters in luminal membrane of ductal cells
301 in salivary glands (Sabino-Silva *et al.*, 2013) highlight the need to evaluate other
302 biomarkers in saliva.

303 Although we have shown that ATR-FTIR technology is useful for the
304 identification of possible biomarkers for monitoring diabetes mellitus in the saliva of rats,

305 this is a first exploratory study using ATR-FTIR technology for this purpose. Therefore,
306 further studies are needed to validate the suggested spectral biomarkers in humans and to
307 determine the applicability of this technique for the monitoring of diabetes mellitus in
308 human saliva. It is important emphasizes that ATR-FTIR have been used for biofluids
309 analysis, allowing same-day detection and grading of a range of diseases in humans
310 (Hands *et al.*, 2016; Hands *et al.*, 2014; Bonnier *et al.*, 2016; Khaustova *et al.*, 2010; Baker
311 & Faulds, 2016; Smith *et al.*, 2016). Also, one limitation of this study is the inclusion of
312 rats in higher levels of glycemia, which was not intentional but could be explained by
313 effect of streptozotocin on beta cells.

314 In conclusion, we showed that ATR-FTIR spectroscopy in saliva is able to
315 differentiate diabetic from non-diabetic and insulin-treated diabetic rats. Our data suggest
316 specific fingerprint regions (highlighted two salivary spectral modes 1452 cm⁻¹ and 836
317 cm⁻¹) capable of discriminating between hyperglycemic and normoglycemic conditions
318 (insulin treated or not) in univariate analysis. A very high discriminatory accuracy of
319 95.2% was also obtained for classifying infrared spectra of saliva between diabetic, non-
320 diabetic and insulin-treated rats by the PCA-LDA and HCA multivariate models. In
321 summary, these salivary results indicate that ATR-FTIR spectroscopy coupled with
322 univariate or multivariate chemometric analysis has the potential to provide a novel non-
323 invasive approach to diabetes monitoring assisting medical decision making to avoid
324 under-treatment or over-treatment with insulin.

325

326 **Methods**

327

328 *Animals*

329 This study was carried out in accordance with recommendations in the Guide for
330 the Care and Use of Laboratory Animals of the Brazilian Society of Laboratory Animals
331 Science (SBCAL). All experimental procedures for the handling, use and euthanasia were
332 approved by the Ethics Committee for Animal Research of the Federal University of
333 Uberlandia (UFU) (License #CEUA-UFU No. 013/2016) according to Ethical Principles
334 adopted by the Brazilian College of Animal Experimentation (COBEA). All effort was
335 taken to minimize the number of animals used and their discomfort.

336 Male wistar rats (~250g) were obtained from Center for Bioterism and
337 Experimentation at the Federal University of Uberlandia. The animals were maintained
338 under standard conditions (22 ± 1 °C, 60% ± 5% humidity and 12-hour light/dark cycles,

339 light on at 7 AM) and were allowed with free access to standard diet and water at the
340 Institute of Biomedical Sciences rodent housing facility.

341

342 ***Induction of Diabetes and insulin treatment***

343 Animals were divided in Non-Diabetic (ND, n = 8), Diabetic (D, n = 6) and
344 diabetic treated with 6U insulin (D6U, n = 7). Diabetes was induced in overnight-fasted
345 animals by an intraperitoneal injection (60 mg/kg) of streptozotocin (STZ) (Sigma-
346 Aldrich, St. Louis, MO. USA) dissolved in 0.1 M citrate buffer (pH 4.5). Animals with
347 hyperglycemia (>250 mg/dl) were chosen as diabetics. Non-diabetic animals received
348 injection of NaCl 0.9% in similar volume.

349 Twenty one days later after induction of diabetes, diabetic rats were submitted to
350 a 7-day treatment with vehicle (ND and D) or with 6U of insulin (D6U) per day (2U at
351 8:30 a.m. and 4U at 5:30 p.m.) subcutaneously (Sabino-Silva *et al.*, 2009). Glucose levels
352 in overnight-fasted were obtained from the tail vein and measured using reactive strips
353 (Accu-Chek Performa, Roche Diagnostic Systems, Basel, Switzerland) by a glucometer
354 (Accu-Chek Performa, Roche Diagnostic Systems, Basel, Switzerland) in the moment of
355 samples collection.

356 In the last day of treatment, the animals were kept in metabolic cages and water
357 intake, food intake, urine volume were measured. Urine was collected over 24 h and the
358 glucose concentration in the urine was evaluated using an enzymatic Kit (Labtest
359 Diagnóstica SA, Brazil). Besides that, variation of gain/loss body weight (Δ body weight)
360 compared parameters in STZ or vehicle induction with parameters after insulin or vehicle
361 treatment.

362

363 ***Saliva collection***

364 After 7-days of treatment, the animals were anaesthetized by an intraperitoneal
365 injection with ketamine (100 mg/kg) and xylazine (20 mg/kg). Stimulated saliva was
366 collected with parasympathetic stimulation through pilocarpine injection (2 mg/kg, i.p.).
367 Stimulated saliva was collected in pre weighed flasks for 10 min from the oral cavity
368 (Sabino-Silva *et al.*, 2013). The collected saliva was stored at -80°C for further processing
369 and analysis.

370

371 ***Chemical profile in stimulated saliva by ATR-FTIR Spectroscopy***

372 Salivary spectra were recorded in 3000 cm⁻¹ to 400 cm⁻¹ region using ATR-FTIR
373 spectrophotometer Vertex 70 (Bruker Optics, Reinstetten, Germany) using a micro-
374 attenuated total reflectance (ATR) component. The crystal material in ATR unit was a
375 diamond disc as internal-reflection element. The salivary pellicle penetration depth
376 ranges between 0.1 and 2 μm and depends on the wavelength, incidence angle of the beam
377 and the refractive index of ATR-crystal material. In the ATR-crystal the infrared beam is
378 reflected at the interface toward the sample. Saliva was directly dried using airflow on
379 ATR-crystal for 2 min before salivary spectra recorded. The air spectra was used as a
380 background in ATR-FTIR analysis. Sample spectra and background was taken with 4 cm⁻¹
381 of resolution and 32 scans were performed for salivary analysis.

382

383 ***Spectra data evaluation procedures***

384 The spectra data obtained were processed using Opus 6.5 software (Bruker Optics,
385 Reinstetten, Germany). Measurements were performed in mid-infrared region (3000–400
386 cm⁻¹) with spectral resolution of 4 cm⁻¹ and 32 scans per spectrum. Samples were pressed
387 into ATR diamond crystal with standardized pressure. For the generation of mean spectra
388 and band areas, the spectra were normalized by vector and baseline corrected to avoid
389 errors during the sample preparations and spectra analysis. To evaluate the mean values
390 for the peak positions, band area of the spectra were considered belonging to each animal
391 of the groups. The band positions were measured using the frequency corresponding to
392 the center of weight of each band. Band areas were calculated from normalized and
393 baseline corrected spectra using OPUS software. Sensitivity and specificity values were
394 calculated based on the external test set as follows:

395 The specificity or true negative rate is defined as the percentage of rats who are correctly
396 identified as being normoglycemic Non-Diabetic (ND) or normoglycemic diabetic treated
397 with 6U insulin (D6U):

$$398 \text{ Specificity} = \frac{TN}{TN + FP}$$

399 The quantity 1-specificity is the false positive rate and is the percentage of rats that are
400 incorrectly identified as diabetic (D).

401 The sensitivity or true positive rate is defined as the percentage of rats who are correctly
402 identified as diabetic (D):

$$403 \text{ Sensitivity} = \frac{TP}{TP + FN}$$

404 where TP stands for true positives; TN for true negatives; FP for false positives; and FN
405 for false negatives.

406

407

408 ***Principal component analysis followed by linear discriminant analysis (PCA-LDA) and***
409 ***Hierarchical Cluster Analysis (HCA)***

410 The principal components were calculated using a full range of the FT-IR spectra
411 (ND, D and DU6) between 3700 and 500 cm⁻¹, and a covariance matrix. The first step
412 was normalization followed by mean centering, the data were analyzed using the principal
413 components analysis (PCA). In this study, the first six principal components (PC1-PC6)
414 were used to perform the linear discriminant analysis (LDA) with leave-one-out cross-
415 validation, according to the pathological reports.

416 Infrared spectra of saliva samples were also analyzed by OPUS software (version
417 4.2) using hierarchical cluster analysis with first-derivative of the training data set. The
418 Dendrogram was performed by Ward's clustering algorithm in the defined spectral
419 regions.

420

421 ***Statistical analysis***

422 The data of the band area were analyzed using the one-way analysis of variance
423 (ANOVA), followed by Tukey Multiple Comparison as a *post-hoc* test. The correlation
424 between values of blood glucose concentration and salivary band areas of the spectra were
425 analyzed by the Pearson correlation test. For all spectral band candidates, we constructed
426 the Receiver Operating Characteristic (ROC) curve and computed the area under the
427 curve (AUC) value, sensitivity and specificity by numerical integration of the ROC curve.
428 The Kolmogorov-Smirnov test was applied to test the normality of the variables. All these
429 analyses were performed using the software GraphPad Prism (GraphPad Prism version
430 7.00 for Windows, GraphPad Software, San Diego, CA, USA). Only values of $p < 0.05$
431 were considered significant and the results were expressed as mean \pm S.D.

432

433 ***Acknowledgements***

434

435 This research was supported by a grant from CAPES/CNPq (#458143/2014), FAPEMIG
436 (#APQ-02872-16) and National Institute of Science and Technology in Theranostics and
437 Nanobiotechnology (CNPq Process N.: 465669/2014-0). CAIXETA, D.C.; AGUIAR, E.

438 M. G.; and CARDOSO-SOUZA, L. received a fellowship from FAPEMIG, CNPq e
439 CAPES, respectively. We would like to thank our collaborators at the Dental Research
440 Center in Biomechanics, Biomaterials and Cell Biology (CPbio).

441

442 References

443

444 ABD-ELRAHEEM, S. E.; EL SAEED, A. M.; MANSOUR, H. H. Salivary changes in
445 type 2 diabetic patients. **Diabetes Metab Syndr**, v. 11 Suppl 2, p. S637-s641, Dec 2017.
446 ISSN 1871-4021.

447

448 ASHCROFT, F. M.; RORSMAN, P. Diabetes mellitus and the beta cell: the last ten years.
449 **Cell**, v. 148, n. 6, p. 1160-71, Mar 16 2012. ISSN 0092-8674.

450

451 BAJAJ, S. et al. Oral manifestations in type-2 diabetes and related complications. **Indian**
452 **J Endocrinol Metab**, v. 16, n. 5, p. 777-9, Sep 2012. ISSN 2230-9500.

453

454 BAKER, Matthew J.; FAULDS, Karen. Fundamental developments in clinical infrared
455 and Raman spectroscopy. **Chemical Society Reviews**, v. 45, n. 7, p. 1792-1793, Apr
456 2016. ISSN 0306-0012

457

458 BELLISOLA, G.; SORIO, C. Infrared spectroscopy and microscopy in cancer research
459 and diagnosis. **Am J Cancer Res**, v. 2, n. 1, p. 1-21, 2012. ISSN 2156-6976.

460

461 BENCHARIT, S. et al. Salivary proteins associated with hyperglycemia in diabetes: a
462 proteomic analysis. **Molecular bioSystems**, v. 9, n. 11, p. 2785-2797, 2013. ISSN 1742-
463 2051

464 BONNIER, Franck et al. Screening the low molecular weight fraction of human serum
465 using ATR-IR spectroscopy. **Journal of biophotonics**, v. 9, n. 10, p. 1085-1097, Oct
466 2016. ISSN: 1864-063X

467

468 BORDER, M. B. et al. Exploring salivary proteomes in edentulous patients with type 2
469 diabetes. **Mol Biosyst**, v. 8, n. 4, p. 1304-10, Apr 2012. ISSN 1742-2051.

470

471 CAETANO JÚNIOR, P. C.; STRIXINO, J. F.; RANIERO, L. Analysis of saliva by
472 Fourier transform infrared spectroscopy for diagnosis of physiological stress in athletes.
473 **Research on Biomedical Engineering**, v. 31, p. 116-124, 2015. ISSN 2446-4740.
474 Disponível em: < http://www.scielo.br/scielo.php?script=sci_arttext&pid=S2446-47402015000200116&nrm=iso >.

476

477 DESAI, G. S.; MATHEWS, S. T. Saliva as a non-invasive diagnostic tool for
478 inflammation and insulin-resistance. **World J Diabetes**, v. 5, n. 6, p. 730-8, Dec 15 2014.
479 ISSN 1948-9358 (Print) 1948-9358.

480
481 DINIZ VILELA, D. et al. The Role of Metformin in Controlling Oxidative Stress in
482 Muscle of Diabetic Rats. **Oxid Med Cell Longev**, v. 2016, p. 6978625, 2016. ISSN 1942-
483 0994. Disponível em: < <https://www.ncbi.nlm.nih.gov/pubmed/27579154> >.

484
485 DOWLATY, N.; YOON, A.; GALASSETTI, P. Monitoring states of altered
486 carbohydrate metabolism via breath analysis: are times ripe for transition from potential to
487 reality? **Curr Opin Clin Nutr Metab Care**, v. 16, n. 4, p. 466-72, Jul 2013. ISSN 1363-
488 1950.

489
490 ELEAZU, C. O. et al. Ameliorative Potentials of Ginger (*Z. officinale Roscoe*) on
491 Relative Organ Weights in Streptozotocin induced Diabetic Rats. **Int J Biomed Sci**, v. 9, n.
492 2, p. 82-90, Jun 2013. ISSN 1550-9702 (Print) 1550-9702.

493
494 GUPTA, A. et al. Evaluation of Correlation of Blood Glucose and Salivary Glucose
495 Level in Known Diabetic Patients. **J Clin Diagn Res**, v. 9, n. 5, p. Zc106-9, May 2015.
496 ISSN 2249-782X (Print)

497 0973-709x.

498
499 GUPTA, S. et al. Comparison of salivary and serum glucose levels in diabetic patients.
500 **J Diabetes Sci Technol**, v. 9, n. 1, p. 91-6, Jan 2015. ISSN 1932-2968.

501 HANDS, James R. et al. Attenuated total reflection Fourier transform infrared
502 (ATR-FTIR) spectral discrimination of brain tumour severity from serum
503 samples. **Journal of biophotonics**, v. 7, n. 3-4, p. 189-199, Apr 2014.
504

505 HANDS, James R. et al. Brain tumour differentiation: rapid stratified serum diagnostics
506 via attenuated total reflection Fourier-transform infrared spectroscopy. **Journal of**
507 **neuro-oncology**, v. 127, n. 3, p. 463-472, May 2016. ISSN 1573-7373 (Print) 0167-594X
508

509 HU, S.; LOO, J. A.; WONG, D. T. Human saliva proteome analysis and disease
510 biomarker discovery. **Expert Rev Proteomics**, v. 4, n. 4, p. 531-8, Aug 2007. ISSN 1478-
511 9450.

512
513 JAVAID, M. A. et al. Saliva as a diagnostic tool for oral and systemic diseases. **J Oral**
514 **Biol Craniofac Res**, v. 6, n. 1, p. 66-75, Jan-Apr 2016. ISSN 2212-4268 (Print) 2212-4268.

515
516 KADASHETTI, V. et al. Glucose Level Estimation in Diabetes Mellitus By Saliva: A
517 Bloodless Revolution. **Rom J Intern Med**, v. 53, n. 3, p. 248-52, Jul-Sep 2015. ISSN 1220-
518 4749 (Print)

519 1220-4749.

520
521 KHAUSTOVA, S. et al. Noninvasive biochemical monitoring of physiological stress by
522 Fourier transform infrared saliva spectroscopy. **Analyst**, v. 135, n. 12, p. 3183-92, Dec 2010.
523 ISSN 0003-2654.

524

525 KUSARI, J. et al. Effect of memantine on neuroretinal function and retinal vascular
526 changes of streptozotocin-induced diabetic rats. **Invest Ophthalmol Vis Sci**, v. 48, n. 11, p.
527 5152-9, Nov 2007. ISSN 0146-0404 (Print) 0146-0404.

528

529 MAHMOUD, S. S. The impact of elevated blood glycemic level of patients with type 2
530 diabetes mellitus on the erythrocyte membrane: FTIR study. **Cell Biochem Biophys**, v. 58,
531 n. 1, p. 45-51, Sep 2010. ISSN 1085-9195.

532

533 MASCARENHAS, P.; FATELA, B.; BARAHONA, I. Effect of diabetes mellitus type 2
534 on salivary glucose--a systematic review and meta-analysis of observational studies. **PLoS**
535 **One**, v. 9, n. 7, p. e101706, 2014. ISSN 1932-6203.

536

537 NAING, C.; MAK, J. W. Salivary glucose in monitoring glycaemia in patients with type
538 1 diabetes mellitus: a systematic review. **J Diabetes Metab Disord**, v. 16, p. 2, 2017. ISSN
539 2251-6581 (Print) 2251-6581.

540

541 NUNES, L. A.; MUSSAVIRA, S.; BINDHU, O. S. Clinical and diagnostic utility of
542 saliva as a non-invasive diagnostic fluid: a systematic review. **Biochem Med (Zagreb)**, v.
543 25, n. 2, p. 177-92, 2015. ISSN 1330-0962 (Print)

544 1330-0962.

545

546 OJEDA, J. J.; DITTRICH, M. Fourier transform infrared spectroscopy for molecular
547 analysis of microbial cells. **Methods Mol Biol**, v. 881, p. 187-211, 2012. ISSN 1064-3745.

548

549 PUTTASWAMY, K. A.; PUTTABUDHI, J. H.; RAJU, S. Correlation between Salivary
550 Glucose and Blood Glucose and the Implications of Salivary Factors on the Oral Health
551 Status in Type 2 Diabetes Mellitus Patients. **J Int Soc Prev Community Dent**, v. 7, n. 1, p.
552 28-33, Jan-Feb 2017. ISSN 2231-0762 (Print)

553 2231-0762.

554

555 RAO, P. V. et al. Salivary protein glycosylation as a noninvasive biomarker for
556 assessment of glycemia. **J Diabetes Sci Technol**, v. 9, n. 1, p. 97-104, Jan 2015. ISSN 1932-
557 2968.

558

559 RAO, P. V. et al. Proteomic identification of salivary biomarkers of type-2 diabetes. **J**
560 **Proteome Res**, v. 8, n. 1, p. 239-45, Jan 2009. ISSN 1535-3893 (Print) 1535-3893.

561

562 ROLO, A. P.; PALMEIRA, C. M. Diabetes and mitochondrial function: role of
563 hyperglycemia and oxidative stress. **Toxicol Appl Pharmacol**, v. 212, n. 2, p. 167-78, Apr
564 15 2006. ISSN 0041-008X (Print) 0041-008x.

565

566 SABINO-SILVA, R. et al. Na⁺-glucose cotransporter SGLT1 protein in salivary glands:
567 potential involvement in the diabetes-induced decrease in salivary flow. **J Membr Biol**, v.
568 228, n. 2, p. 63-9, Mar 2009. ISSN 0022-2631.

569

570 SABINO-SILVA, R. et al. Increased SGLT1 expression in salivary gland ductal cells
571 correlates with hyposalivation in diabetic and hypertensive rats. **Diabetol Metab Syndr**, v.
572 5, n. 1, p. 64, Oct 24 2013. ISSN 1758-5996 (Print) 1758-5996.

573

574 SAXENA, S. et al. A Review of Salivary Biomarker: A Tool for Early Oral Cancer
575 Diagnosis. **Adv Biomed Res**, v. 6, p. 90, 2017. ISSN 2277-9175 (Print)

576 2277-9175.

577

578 SCOTT, D. A. et al. Diabetes-related molecular signatures in infrared spectra of human
579 saliva. **Diabetol Metab Syndr**, v. 2, p. 48, Jul 14 2010. ISSN 1758-5996.

580

581 SEVERCAN, F. et al. FT-IR spectroscopy in diagnosis of diabetes in rat animal model.
582 **J Biophotonics**, v. 3, n. 8-9, p. 621-31, Aug 2010. ISSN 1864-063x.

583

584 SIMSEK OZEK, N. et al. Differentiation of Chronic and Aggressive Periodontitis by
585 FTIR Spectroscopy. **J Dent Res**, v. 95, n. 13, p. 1472-1478, Dec 2016. ISSN 0022-0345.

586 SMITH, Benjamin R. et al. Combining random forest and 2D correlation analysis to
587 identify serum spectral signatures for neuro-oncology. **Analyst**, v. 141, n. 12, p. 3668-3678,
588 Jun 2016.

589

590

591 SRINIVASAN, M. et al. Literature-based discovery of salivary biomarkers for type 2
592 diabetes mellitus. **Biomark Insights**, v. 10, p. 39-45, 2015. ISSN 1177-2719 (Print) 1177-
593 2719.

594

595 USPSTF. Screening for type 2 diabetes mellitus in adults: U.S. Preventive Services Task
596 Force recommendation statement. **Ann Intern Med**, v. 148, n. 11, p. 846-54, Jun 3 2008.
597 ISSN 0003-4819.

598

599 XIA, J. et al. Translational biomarker discovery in clinical metabolomics: an introductory
600 tutorial. **Metabolomics**, v. 9, n. 2, p. 280-299, Apr 2013. ISSN 1573-3882 (Print)

601 1573-3882.

602

603 YU, M. C. et al. Label Free Detection of Sensitive Mid-Infrared Biomarkers of
604 Glomerulonephritis in Urine Using Fourier Transform Infrared Spectroscopy. **Sci Rep**, v. 7,
605 n. 1, p. 4601, Jul 04 2017. ISSN 2045-2322.

606

607 ZHANG, C. Z. et al. Saliva in the diagnosis of diseases. **Int J Oral Sci**, v. 8, n. 3, p. 133-
608 7, Sep 29 2016. ISSN 1674-2818.

609

610 ZLOCZOWER, M. et al. Relationship of flow rate, uric acid, peroxidase, and superoxide
611 dismutase activity levels with complications in diabetic patients: can saliva be used to
612 diagnose diabetes? **Antioxid Redox Signal**, v. 9, n. 6, p. 765-73, Jun 2007. ISSN 1523-0864
613 (Print) 1523-0864.

614

615 **Table 1.** Effect of diabetes and insulin on body weight, water intake, food intake,
616 glycemia, urine volume and urine glucose concentration.

617

Parameters	ND	D	D6U
Δ Body weight (g)	48.4±8.3	-2.7±11.3*	39.5±12.8#
Water intake (mL)	39.1±3.1	150.6±17.9*	60.0±6.8#
Food intake (g)	18.3±1.3	35.0±4.1*	29.7±2.6*
Glycemia (mg/dL)	83.2±4.2	497.6±19.6*	81.0±19.2#
Urine volume (mL)	22.1.6±3.4	128.9±8.6*	40.7±7.1#
Urine glucose (mg/dL)	24.7±7.2	337.2±15.8*	148.0±34.6*#

618

619

620

621

622

623

624

625

626

627

628

629

630

631

632

633

634

635

636

637

638

639

640

641 **Supplementary Table 1.** Mean quadratic distance in saliva of ND, D and D6U rats.

642

Quadratic distance	ND	D	D6U
D	0,0000	23,3348	37,2085
D6U	23,3348	0,0000	11,5541
ND	37,2085	11,5541	0,0000

643

644

645

646

647

648

649

650

651

652

653

654

655

656

657

658

659

660

661

662

663

664

665

666

667

668

669

670 **Supplementary Table 2.** Discriminant linear function in saliva of ND, D and D6U rats.

	ND	D	D6U
Constant	-7,105	-1,663	-3,374
CP1	20,686	1,288	-16,659
CP2	34,740	-8,064	-19,007
CP3	18,897	-0,100	-14,095
CP4	-3,054	5,305	-2,359
CP5	4,356	-9,836	5,357
CP6	5,835	-0,779	-3,699

671

672

673

674

675

676

677

678

679

680

681

682

683

684

685

686

687

688

689

690

691

692

693

694 **Supplementary Table 3.** Summary of classification with the quadratic distance of each
 695 sample, prediction, validation and probability of each sample in saliva of ND, D and D6U
 696 rats.

Sample	True group	Predicted group	Val-X			Quadratic distance	Probability	
			Group	Group	Pred.		Predicted	Val-X
1	ND	ND	ND	D	58.073	72.570	0.00	0.00
				D6U	23.160	29.507	0.00	0.00
				ND	6.079	12.211	1.00	1.00
2	ND	ND	ND	D	36.580	34.838	0.00	0.00
				D6U	11.348	11.078	0.03	0.14
				ND	4.371	7.464	0.97	0.86
3	ND	ND	ND	D	35.359	33.417	0.00	0.00
				D6U	10.335	9.816	0.02	0.07
				ND	2.961	4.497	0.98	0.93
4	ND	ND	ND	D	33.837	31.958	0.00	0.00
				D6U	20.628	22.550	0.00	0.00
				ND	3.528	5.608	1.00	1.00
5	ND	ND	ND	D	63.675	88.572	0.00	0.00
				D6U	34.276	54.739	0.00	0.00
				ND	6.646	14.182	1.00	1.00
6	ND	ND	ND	D	29.741	28.369	0.00	0.00
				D6U	9.677	9.203	0.05	0.16
				ND	3.678	5.918	0.95	0.84
7	ND	ND	ND	D	40.529	38.586	0.00	0.00
				D6U	8.646	8.220	0.02	0.03
				ND	1.065	1.409	0.98	0.97
8	ND	ND	ND	D	31.222	29.651	0.00	0.00
				D6U	5.711	5.542	0.21	0.39
				ND	3.021	4.612	0.79	0.61
9	D	D	D	D	6.582	15.951	1.00	1.00
				D6U	26.329	27.438	0.00	0.00
				ND	42.640	44.320	0.00	0.00
10	D	D	D	D	6.150	14.176	1.00	1.00
				D6U	35.688	42.839	0.00	0.00
				ND	41.710	42.420	0.00	0.00
11	D	D	D	D	4.543	8.862	1.00	1.00
				D6U	24.542	23.925	0.00	0.00
				ND	41.537	41.006	0.00	0.00
12	D	D	D	D	5.014	10.244	1.00	0.99
				D6U	21.611	20.666	0.00	0.01

				ND	41.594	41.372	0.00	0.00
13	D	D	D	D	5.526	11.899	1.00	0.92
				D6U	17.901	16.907	0.00	0.08
				ND	28.636	27.276	0.00	0.00
14	D	D	D	D	9.967	40.402	1.00	1.00
				D6U	51.721	117.859	0.00	0.00
				ND	64.915	127.897	0.00	0.00
15	D6U	D6U	D6U	D	45.891	67.075	0.00	0.00
				D6U	6.835	15.774	1.00	1.00
				ND	22.101	29.173	0.00	0.00
16	D6U	D6U	D6U	D	34.031	36.870	0.00	0.00
				D6U	4.261	7.567	0.88	0.54
				ND	8.291	7.852	0.12	0.46
17	D6U	D6U	D6U	D	31.428	32.102	0.00	0.00
				D6U	3.134	5.055	0.93	0.79
				ND	8.210	7.754	0.07	0.21
18	D6U	D6U	D6U	D	23.558	22.563	0.00	0.00
				D6U	3.718	6.296	0.97	0.87
				ND	10.479	10.037	0.03	0.13
19	D6U	D6U	D6U	D	23.534	22.983	0.00	0.00
				D6U	5.454	10.844	1.00	1.00
				ND	24.905	31.891	0.00	0.00
20	D6U	D6U	D6U	D	29.999	30.895	0.00	0.00
				D6U	4.318	7.707	1.00	1.00
				ND	19.325	21.357	0.00	0.00
21	D6U	D6U	D*	D	13.77	13.15	0.21	1.00
				D6U	11.15	51.72	0.79	0.00
				ND	26.44	62.40	0.00	0.00

697

698

699

700

701

702

703 **Legends**

704

705 **Figure 1.** Average ATR-FTIR spectra (3000-400 cm⁻¹) in saliva of Non-Diabetic rats
706 (ND), diabetic rats (D) and diabetic treated with 6U insulin (D6U).

707

708 **Figure 2.** Spectral of 1452 cm⁻¹ (A); Band area of 1452 cm⁻¹ (B); Pearson correlation
709 between glycemia and band area of 1452 cm⁻¹ (C); ROC curve analyses of 1452 to

710 normoglycemic and hyperglycemic (D); ROC curve analyses of 1452 to diabetic and
711 diabetic treated with insulin (E). Non-diabetic rats (ND), diabetic rats (D) and diabetic
712 treated with 6U insulin (D6U).

713

714 **Figure 3.** Spectral of 836 cm-1 (A); Band area of 836 cm-1 (B); Pearson correlation
715 between glycemia and band area of 836 cm-1 (C); ROC curve analyses of 836 to
716 normoglycemic and hyperglycemic (D); ROC curve analyses of 836 to diabetic and
717 diabetic treated with insulin (E). Non-diabetic rats (ND), diabetic rats (D) and diabetic
718 treated with 6U insulin (D6U).

719

720 **Figure 4.** PCA analyses. Non-diabetic rats (ND), diabetic rats (D) and diabetic treated
721 with 6U insulin (D6U).

722

723 **Figure 5.** HCA analyses. Non-diabetic rats (ND), diabetic rats (D) and diabetic treated
724 with 6U insulin (D6U).

725

726

727 **Supplementary Figure 1.** Spectral of 2924 cm-1 (A); Band area of 2924 cm-1 (B);
728 Pearson correlation between glycemia and band area of 2924 cm-1 (C); ROC curve
729 analyses of 2924 cm-1 to normoglycemic and hyperglycemic (D); ROC curve analyses
730 of 2924 cm-1 to diabetic and diabetic treated with insulin (E). Non-diabetic rats (ND),
731 diabetic rats (D) and diabetic treated with 6U insulin (D6U).

732

733 **Supplementary Figure 2.** Spectral of 1549 cm-1 (A); Band area of 1549 cm-1 (B);
734 Pearson correlation between glycemia and band area of 1549 cm-1 (C); ROC curve
735 analyses of 1549 cm-1 to normoglycemic and hyperglycemic (D); ROC curve analyses
736 of 1549 cm-1 to diabetic and diabetic treated with insulin (E). Non-diabetic rats (ND),
737 diabetic rats (D) and diabetic treated with 6U insulin (D6U).

738

739 **Supplementary Figure 3.** Spectral of 1313 cm-1 (A); Band area of 1313 cm-1 (B);
740 Pearson correlation between glycemia and band area of 1313 cm-1 (C); ROC curve
741 analyses of 1313 cm-1 to normoglycemic and hyperglycemic (D); ROC curve analyses
742 of 1313 cm-1 to diabetic and diabetic treated with insulin (E). Non-diabetic rats (ND),
743 diabetic rats (D) and diabetic treated with 6U insulin (D6U).

744

745 **Supplementary Figure 4.** Spectral of 1120 cm-1 (A); Band area of 1120 cm-1 (B);
746 Pearson correlation between glycemia and band area of 1120 cm-1 (C); ROC curve
747 analyses of 1120 cm-1 to normoglycemic and hyperglycemic (D); ROC curve analyses
748 of 1120 cm-1 to diabetic and diabetic treated with insulin (E). Non-diabetic rats (ND),
749 diabetic rats (D) and diabetic treated with 6U insulin (D6U).

750

751

Figure 1.

bioRxiv preprint doi: <https://doi.org/10.1101/781096>; this version posted September 24, 2019. The copyright holder for this preprint (which was not certified by peer review) is the author/funder, who has granted bioRxiv a license to display the preprint in perpetuity. It is made available under aCC-BY 4.0 International license.

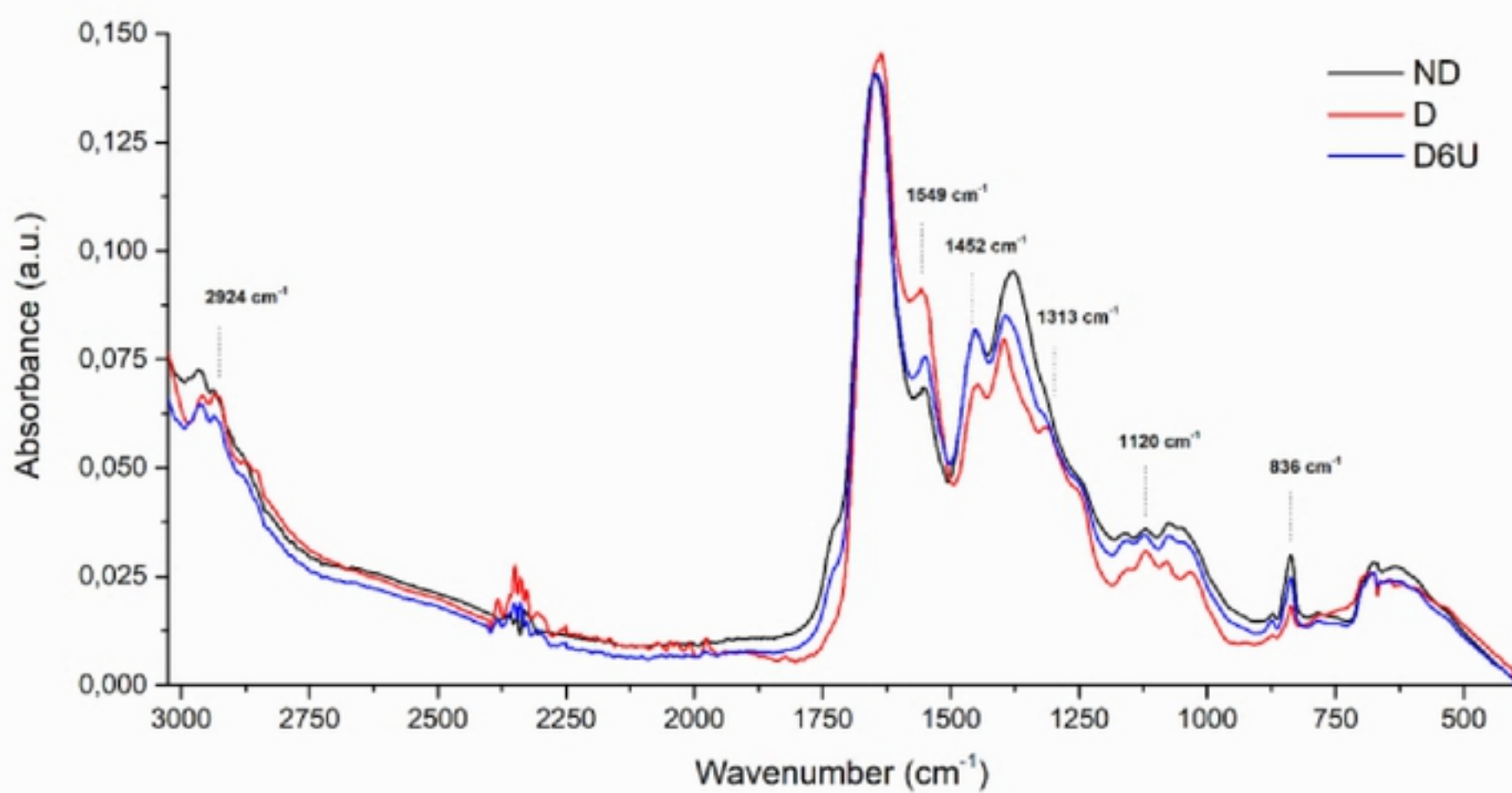


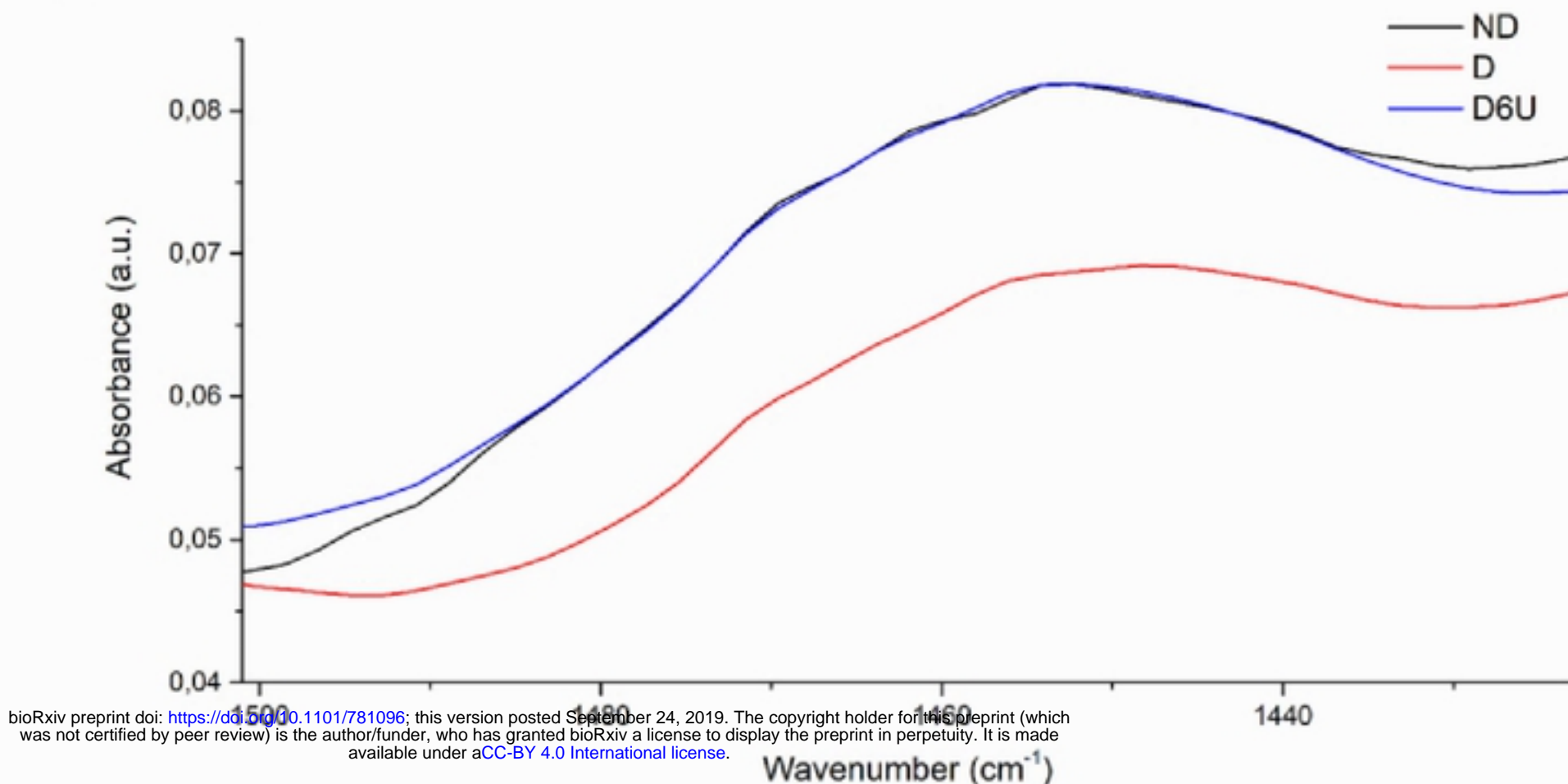
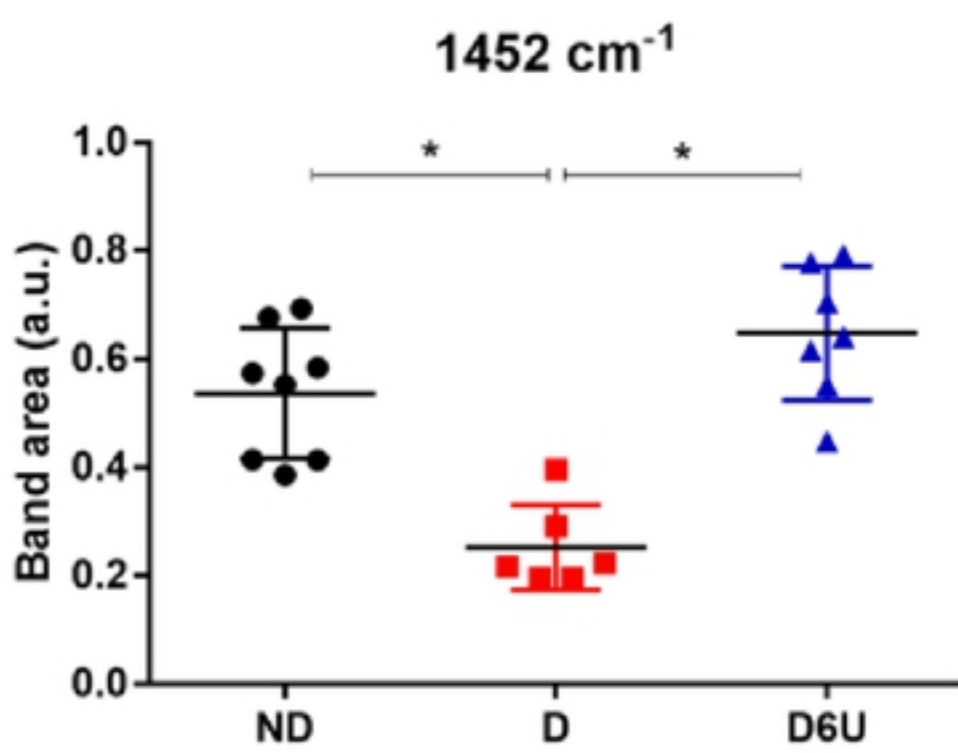
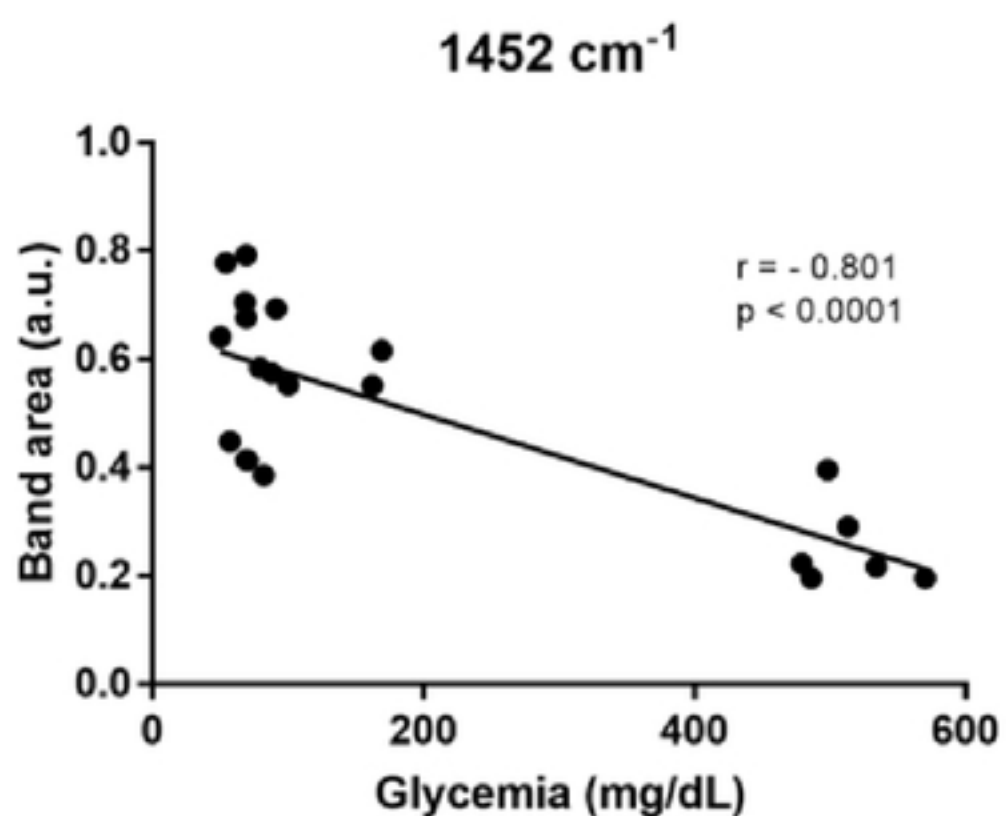
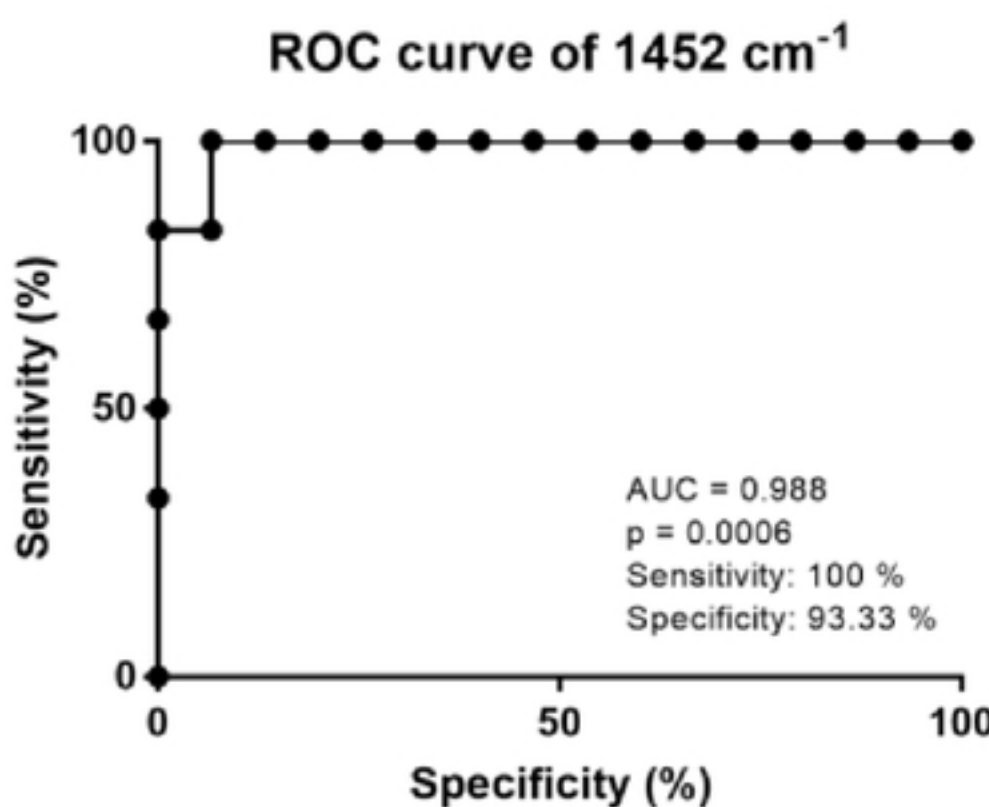
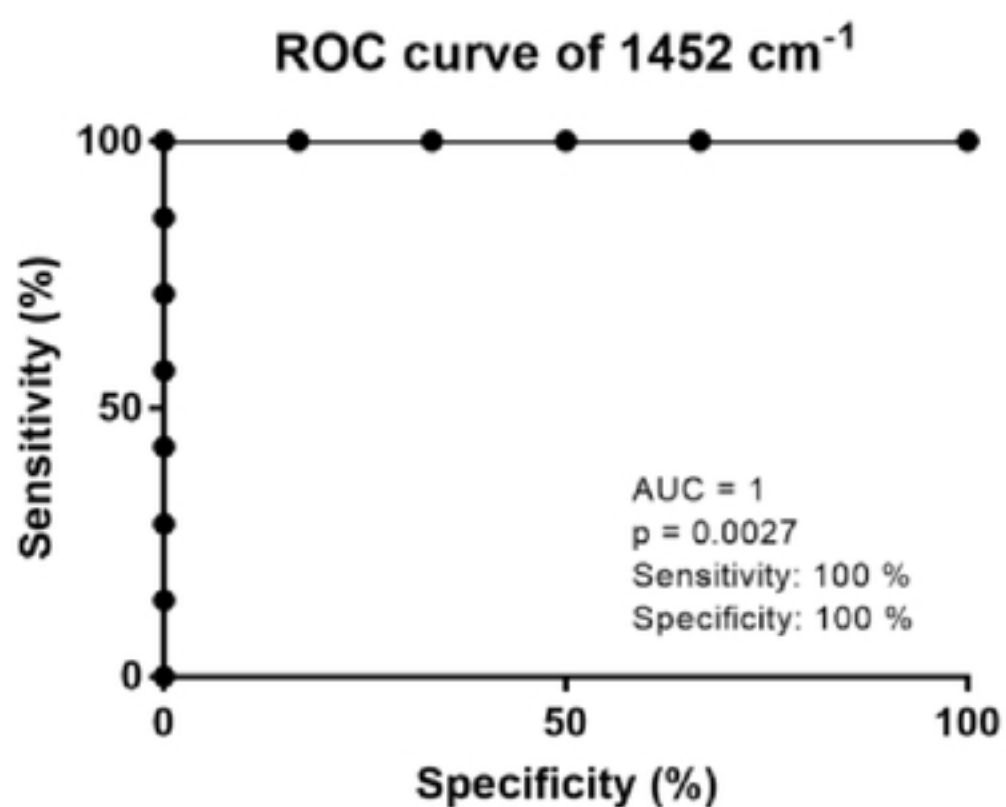
Figure 2.**A****B****C****D****E**

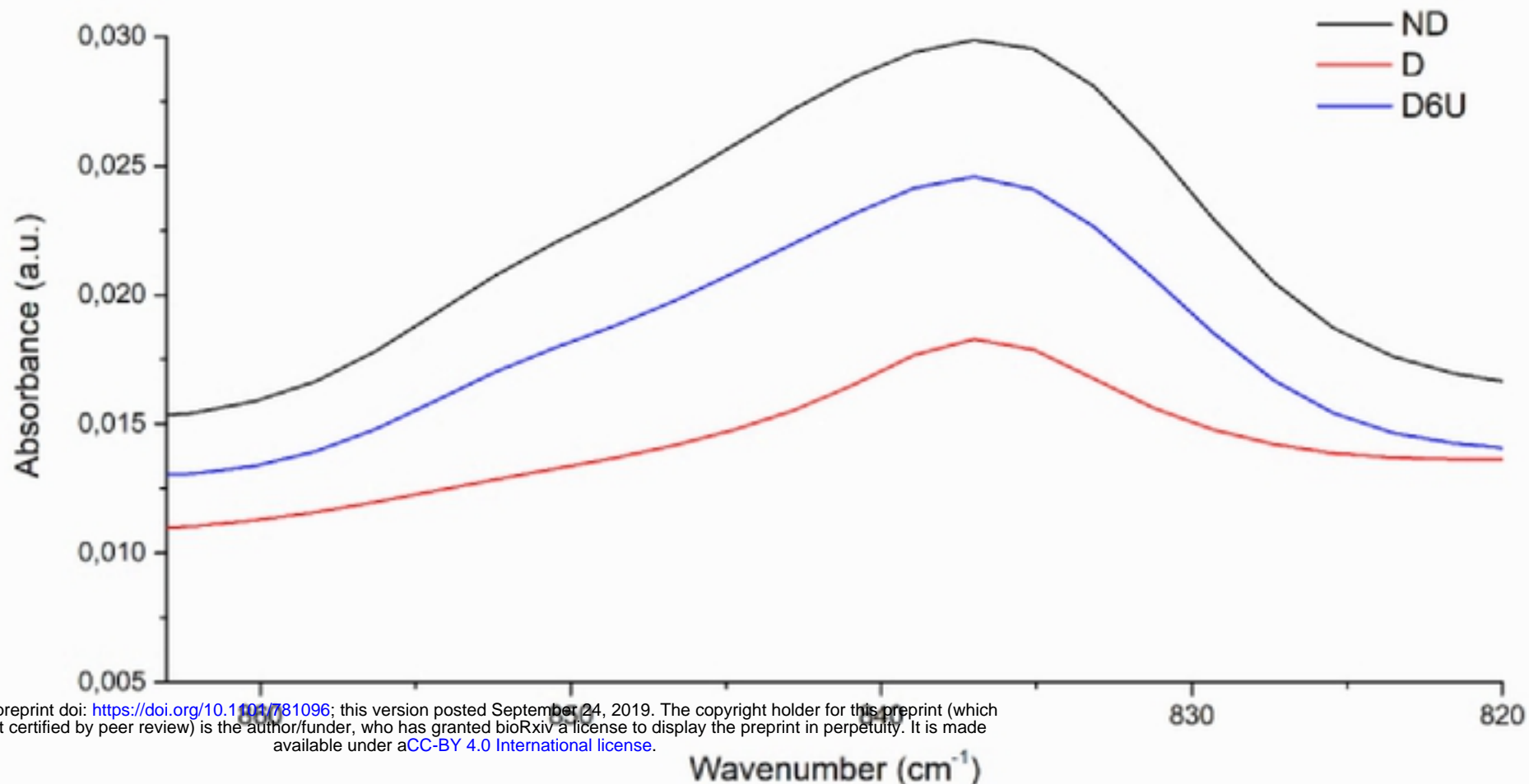
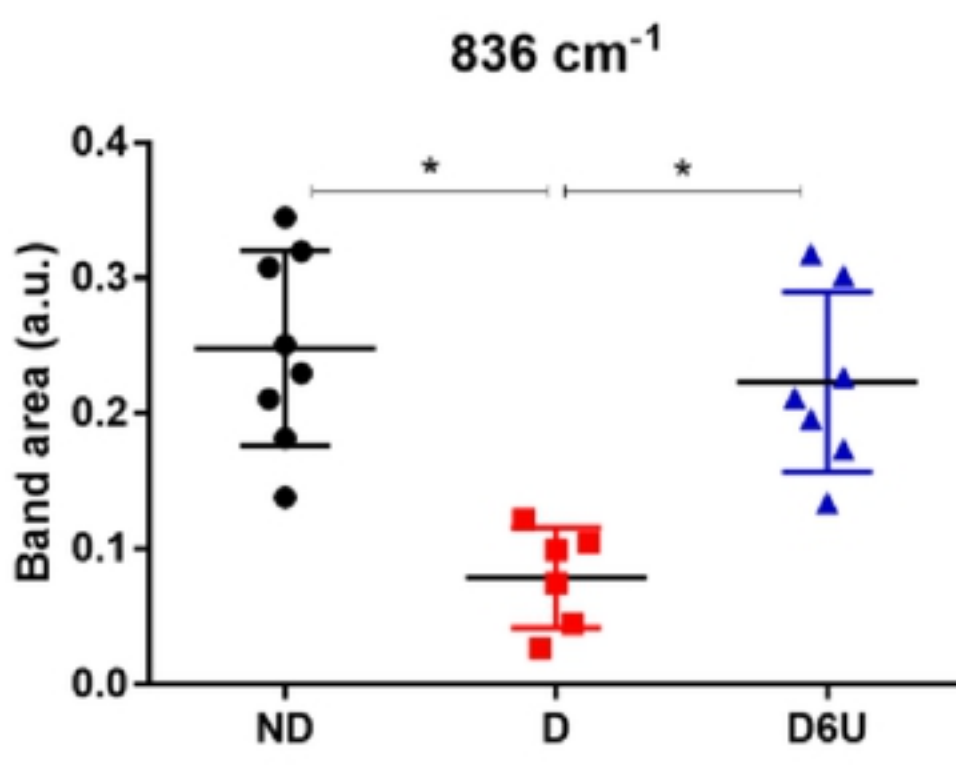
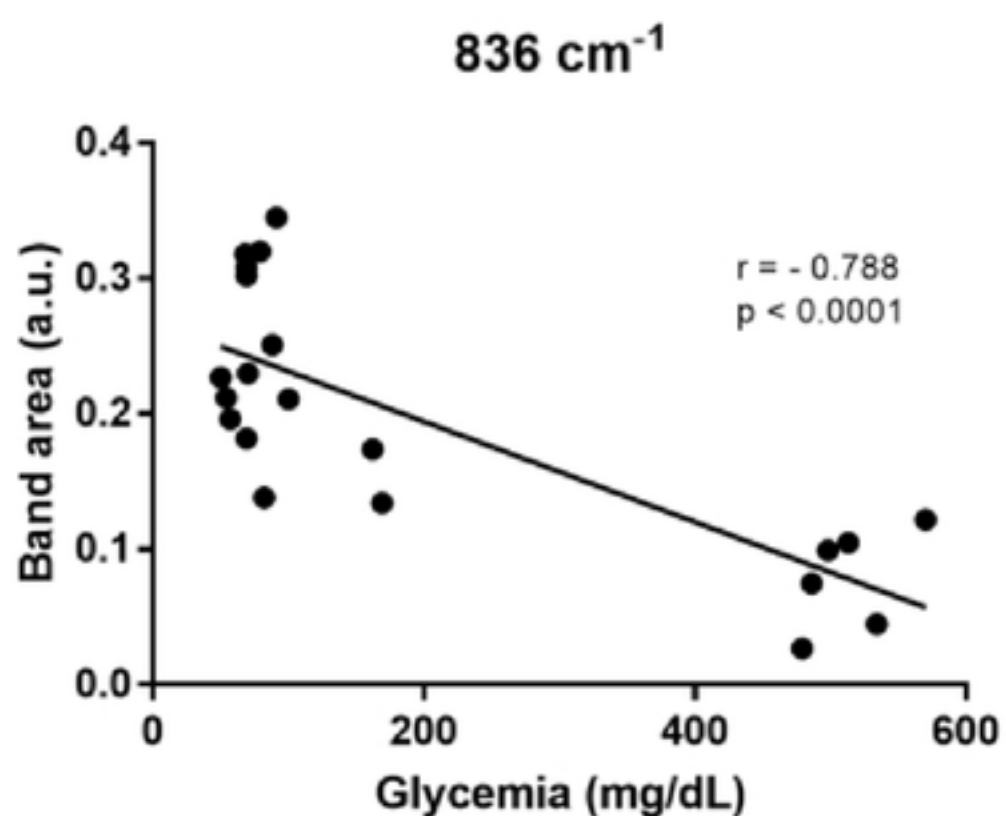
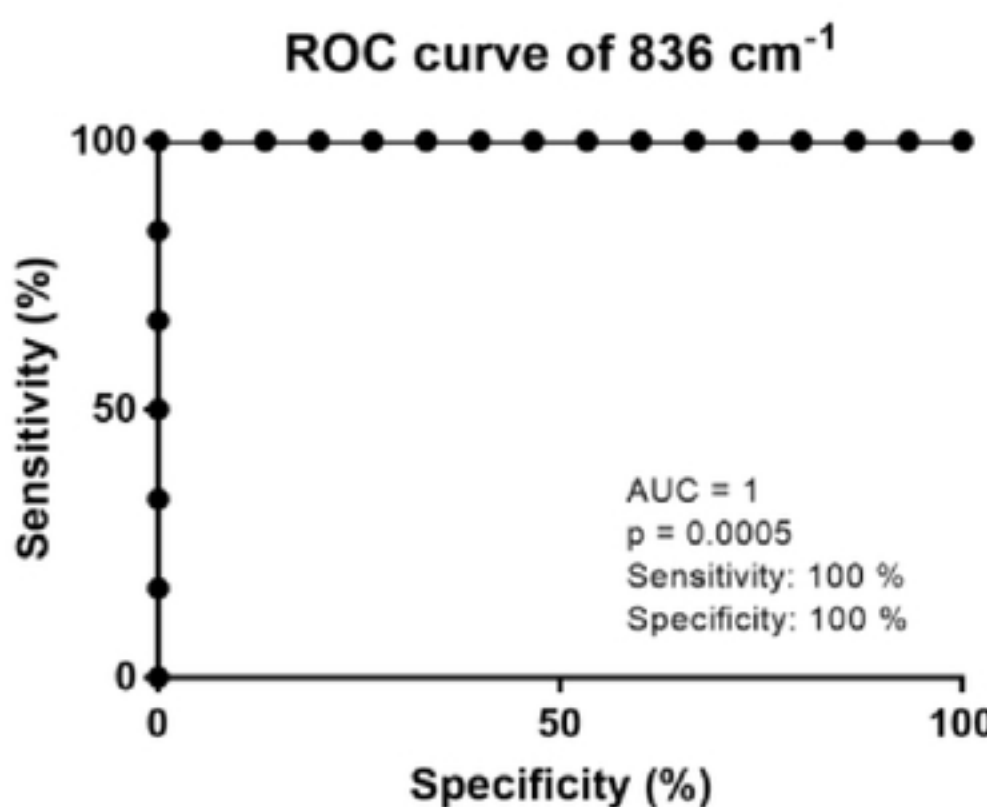
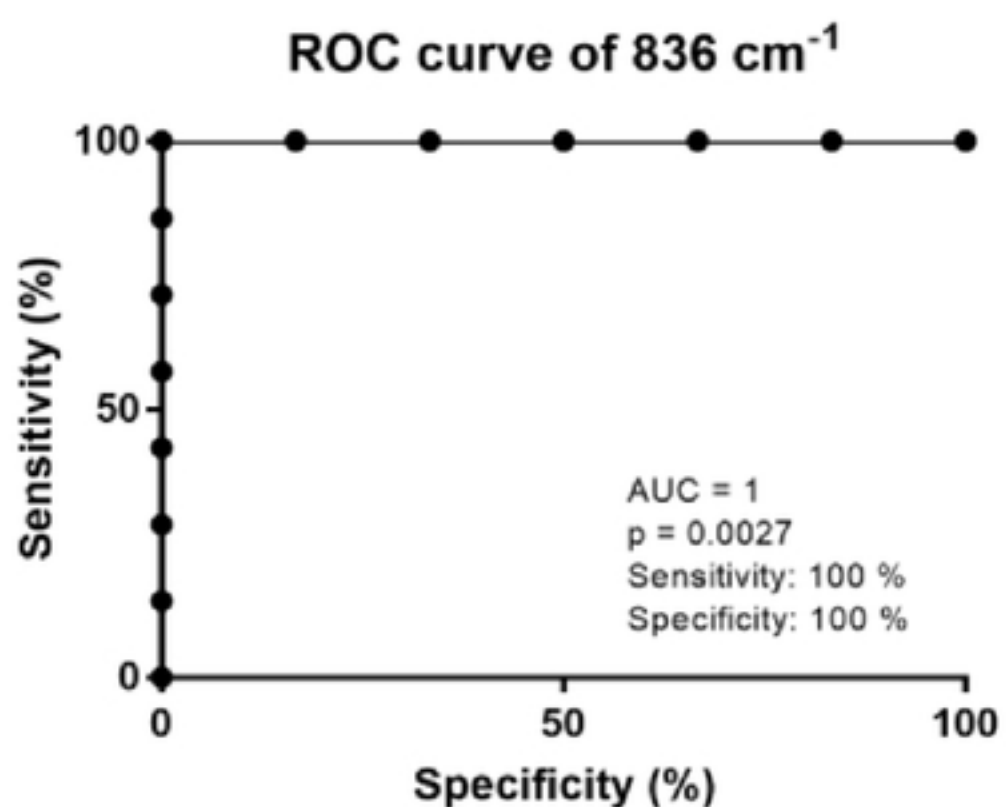
Figure 3.**A****B****C****D****E**

Figure 4.

bioRxiv preprint doi: <https://doi.org/10.1101/781096>; this version posted September 24, 2019. The copyright holder for this preprint (which was not certified by peer review) is the author/funder, who has granted bioRxiv a license to display the preprint in perpetuity. It is made available under aCC-BY 4.0 International license.

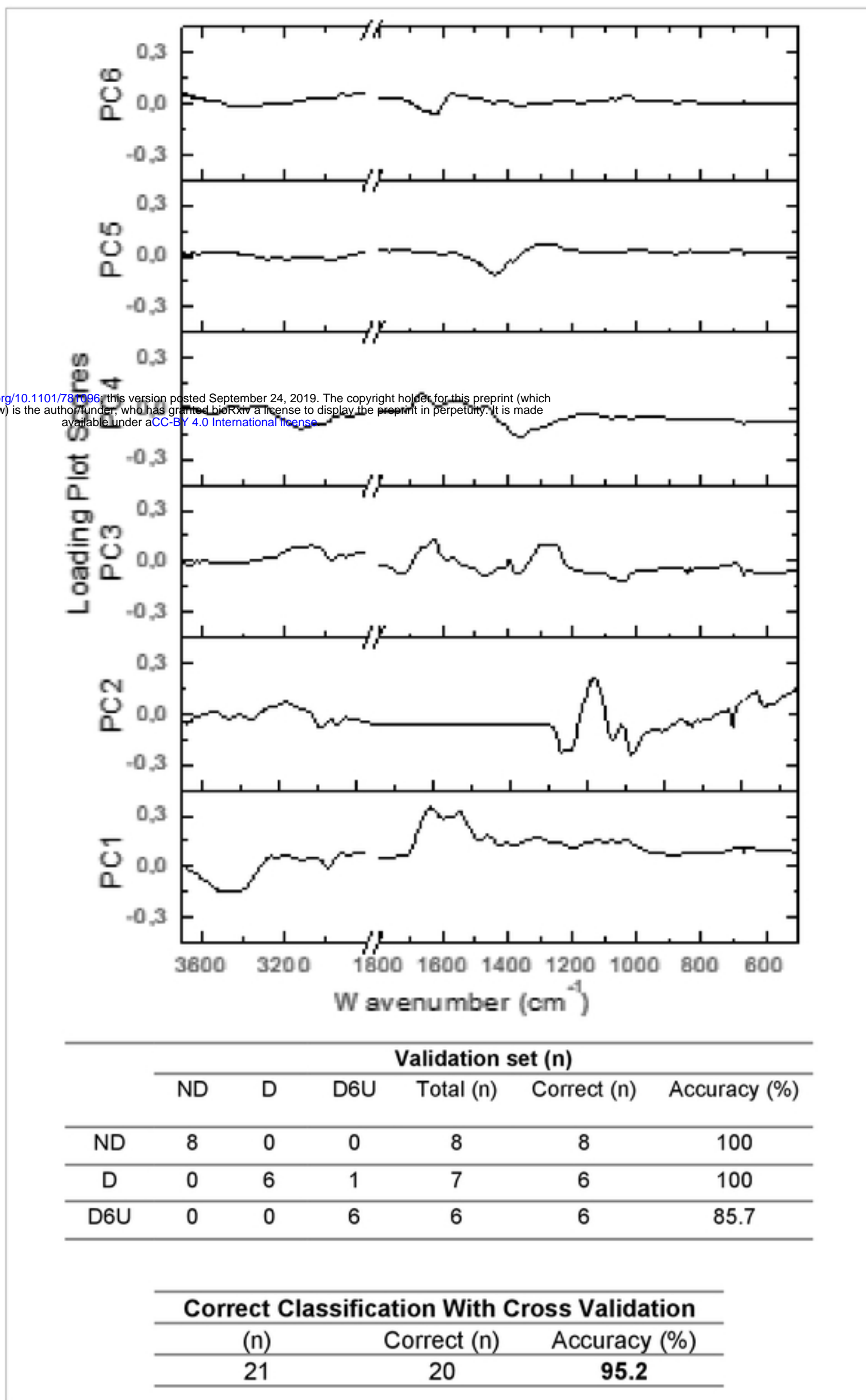


Figure 5.

